

Optical density analysis in autoradiographic images from BNCT protocols

C. Vidal^a, A. Portu^{b,c}, S.I. Thorp^b, P. Curotto^b, E. Pozzi^b, G. Saint Martin^{b,d,*}

^a Facultad de Ingeniería, Universidad Favaloro, Tte. Gral. J. D. Perón 3175, Ciudad Autónoma de Buenos Aires, Argentina

^b Comisión Nacional de Energía Atómica, Av. Gral. Paz 1499. San Martín, Buenos Aires, Argentina

^c Consejo Nacional de Investigaciones Científicas y Técnicas, Godoy Cruz 2290, Ciudad Autónoma de Buenos Aires, Argentina

^d Instituto Jorge Sábato, Universidad Nacional de San Martín, Av. Gral. Paz 1499. San Martín, Buenos Aires, Argentina



ARTICLE INFO

Keywords:

Neutron autoradiography
Boron microdistribution
Optical density
BNCT
Grey level

ABSTRACT

In Boron Neutron Capture Therapy (BNCT) research, information on spatial distribution and concentration of boron in tissues is essential for the treatment planning and for dose determination. Neutron autoradiography technique offers the possibility to gain insight into boron biodistribution in tissues. The irradiation of tissue sections deposited on nuclear track detectors produces damages in the latter, which can be visualized by microscope imaging and that are spatially correlated with the boron localization in the biological section. We had previously developed a methodology for the quantification of boron concentration in tissue samples by nuclear track density determination (QTA).

In this work we analyzed the optical density (OD) in autoradiographic images where track density is too high to be quantified by track counting. OD was determined from grey level measurements on low magnification micrographs and proved to be a suitable parameter to quantify boron concentration. The images were originated by placing polycarbonate detectors in contact with samples containing ¹⁰B atoms, irradiated with thermal neutrons and finally chemically attacked. Reference standards were developed from aqueous solutions prepared with known boron concentrations in order to construct calibration curves. The obtained optical density values were compared with curves proposed by other authors, showing similar tendencies. The calibration curve was used to make preliminary boron concentration determinations in histological tissue sections of animals infused with boron compounds, which agreed with measurements realized by the QTA approach.

The methodology proposed in this work would allow a fast preliminary analysis of histological and autoradiographic images in samples of interest for BNCT.

1. Introduction

BNCT is a binary radiation treatment modality which potentially targets cancer cells in a selective way. A non-toxic compound containing atoms of the stable isotope of boron (¹⁰B) is preferentially incorporated into tumor cells. The boron neutron capture reaction ¹⁰B(n,α)⁷Li occurs when the tissue is exposed to a thermal neutron flux and the resulting ions (alpha particles and recoiling ⁷Li nuclei) deposit most of their energy within the ¹⁰B-containing cells. In this way, individual cancer cells would suffer a lethal damage, sparing the surrounding normal tissue (Moss, 2014).

BNCT has been used as a treatment for glioblastoma multiforme, head and neck tumors and melanoma in several countries, with promising results (e.g. Kato et al., 2004; Gonzalez et al., 2004; Wang et al., 2011; Kankaanranta et al., 2012). Clinical trials have also been performed in liver metastases, lung metastases and osteosarcoma (e.g.

Zonta et al., 2006; Suzuki et al., 2006; Yanagie et al., 2014; Futamura et al., 2014).

The precise knowledge of the boron compounds location in tumor and surrounding tissue is essential to optimize the treatment protocol, taking into account that different tissue structures will accumulate different amounts of boron, thus affecting dose distribution.

The determination of the concentration and distribution in a material, of elements emitting heavy particles (e.g., ¹⁰B) can be performed by analyzing the autoradiography image of the sample in a nuclear track detector (NTD). This is the case of biological samples coming from BNCT (Boron Neutron Capture Therapy) protocols. Nuclear tracks are produced by Li ions and alpha particles resulting from the neutron capture reaction when the sample-detector assembly is irradiated with thermal neutrons (Portu et al., 2013). In our laboratory, a quantitative autoradiography technique has been developed for the measurement of ¹⁰B concentration, based on counting the nuclear tracks generated from

* Corresponding author. Comisión Nacional de Energía Atómica, Av. Gral. Paz 1499. San Martín, Buenos Aires, Argentina.
E-mail address: gisaint@cenea.gov.ar (G. Saint Martin).

tissue sections deposited on the detector (Portu et al., 2011a, 2015). When the number of tracks is considerable, the NTD enters a saturated regime and the usual track-counting methods cannot be applied because of track overlapping (Portu et al., 2011b). In this case another approach, that takes advantage of the collective effect produced by tracks in the detector should be assessed. In particular, the optical properties of the etched foil change visibly, and light transmission could be considered for this purpose.

On the other hand, a rough overview of the compound uptake in the different tissue structures could be useful. It would be interesting to have a method based on an easy-to-measure property, and use it to determine the boron concentration.

For this purpose, samples can be irradiated with higher fluence (10^{13} n.cm⁻²) and etched for a longer time. In this way the tracks overlap to form a continuous image, allowing for the analysis and quantification of the grey levels.

To perform this analysis, a code in C# (BNCT-AR) was developed, that allows easy and rapid estimation of both the distribution and concentration of boron for high fluence images (Vidal et al., 2015). The BNCT-AR code calculates the boron concentration in a certain region of the sample by evaluating the grey levels of the autoradiographic image and using a calibration curve. The program also includes the necessary tools to edit and modify images acquired with the microscope, in order to facilitate their analysis. In addition, it manages the storage of the generated studies in a database developed for this purpose. The use of low magnification images allows the exploration of all the regions of interest (ROIs) in only one image.

Grey levels (NG) with values in a range from 0 to 255, can be used as a parameter that accounts for light transmission, which can be modeled considering that the image is formed by a two-dimensional array of visible tracks on the surface of the detector, as proposed in Ilic and Najzer's works (Ilic and Najzer, 1990a, 1990b). Optical density, according to the Beer-Lambert law (Swinehart, 1962), is defined as

$$OD = \log \frac{I_0}{I} = -\log T \quad (1)$$

where T is the light transmission, I_0 is the original intensity and I is the resulting intensity after crossing the sample. It can be assumed that for a given detector and type of charged particles, OD is mainly determined by track density ρ (or number of tracks per unit area), by track size, and by the optical properties of each individual track. NG can be taken as the grey level associated to transmitted light I, thus, OD can be calculated with measured NG through equation (1a).

$$OD = \log \frac{NG_0}{NG} \quad (1a)$$

NG_0 is the grey level corresponding to a control foil without autoradiographic image.

When analyzing this type of autoradiographic images, a higher concentration of boron in the tissue implies a higher density of tracks in the detector, and therefore a lower intensity of light is transmitted. That

is, OD increases with boron concentration.

In this work, images corresponding to standard samples with a known concentration of ¹⁰B were analyzed, and the response in terms of grey level NG/optical density OD was analyzed as a function of concentration. In addition, the exposure parameter (E) proposed in the literature (Ilic and Najzer, 1990a, 1990b; Skvarc et al., 1999) is defined as

$$E = A_t \cdot \rho \quad (2)$$

where A_t is the average area of tracks and ρ is track density. It was used to compare our results with curves obtained by the model developed by Ilic and Najzer (1990a) for thick detectors, namely those detectors in which thickness of the residual foil is greater than the depth of tracks after chemical attack (Equation (3)).

$$OD = -\log [T_f e^{-E} + T_{11} (1 - e^{-\rho \pi r_{11}^2}) + T_{12} (e^{-\rho \pi r_{11}^2} - e^{-E})] \quad (3)$$

In Equation (3), T_{11} and T_{12} are parameters related to light transmission in an individual track. Though light transmission depends on track radius, an approximation is made in the model for thick plastic detectors in which two concentric regions with constant OD in each of them are considered. In this model r_{11} is the radius of the inner region in the track image at the light microscope. Values of the above parameters reported by Ilic and Najzer (1990a) were used to calculate theoretical curves.

Curves of boron concentration as a function of the optical density, included in the BNCT-AR code, were used to analyze biological samples and an example of the preliminary results is presented in this work.

2. Materials and methods

Foils of transparent 250 μ m thickness polycarbonate (Lexan™) were used as NTD. They were put in contact with two types of standard samples:

- 1) Enriched boric acid (99%) solutions with known concentration, between 0 and 200 ppm. They were injected in Small Lexan Cases, SLCs, (Portu et al., 2011a). A schematic of the SLC is shown in Fig. 1a).
- 2) Agarose gels (Low Melting Point: 65.5 °C, Promega™), prepared with solutions of boric acid as in 1). The agarose gel was poured directly onto a Lexan foil, and on this gel still in "liquid" state a second Lexan foil was placed. In this way the gel solidified between two polycarbonate foils. This process was schematized in Fig. 1b).

The samples were irradiated at the central thermal column facility of the RA-3 (Ezeiza Atomic Center) reactor with a thermal neutron fluence of 10^{13} n.cm⁻². Then the detectors were etched with PEW solution (30 g KOH + 80 g ethyl alcohol + 90 g distilled water) at 70 °C for 4 and 5 min. Images were acquired with an Olympus DP70 microscope equipped with a CCD camera, with an original magnification of

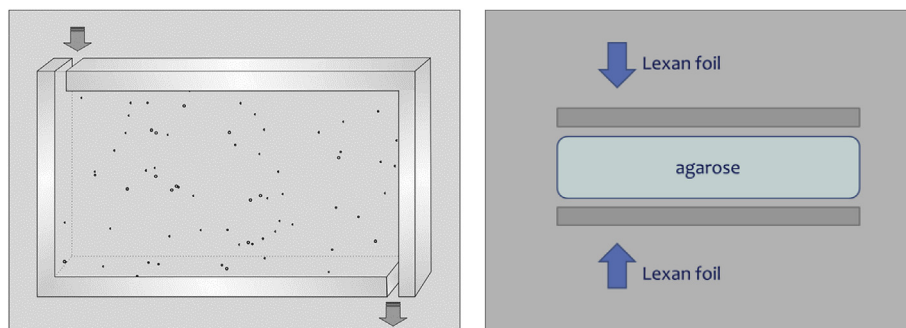


Fig. 1. a) Aqueous solutions of enriched boric acid (99%) in Small Lexan™ Cases. Adapted from Portu et al. (2011a); b) Low Melting point agarose gel in between two Lexan foils.

1.25 ×.

The average value of the track area (A_t) had to be determined in order to calculate Exposure. A_t was measured in foils corresponding to SLCs filled with boric acid solution (50 ppm), irradiated with $\phi = 10^{12}$ n.cm⁻² fluence, and etched for 4 and 5 min. Track diameters were determined with 100 × original magnification, using a calibrated grid. Grey levels were measured with the BNCT-AR software.

In order to calculate the optical density, NG_0 had to be measured. Ideally, in a scale from 0 to 255, a sample with no boron content should generate a NG_0 equal to 255. In practice, the detector thickness generates reflection and refraction of light, which reduces this value. We have found that for our detectors and experimental conditions this value is typically, $NG_0 = 169$. The biological samples used for preliminary determinations of boron concentration in tissue correspond to premalignant tissue of hamster cheek pouch (e.g. Kreimann et al., 2001). The hamster had been infused with a boronated compound (GB-10: Na₂[closo-B₁₀H₁₀], 50 mg kg⁻¹) and sacrificed 3 h post administration, according to the protocol reported elsewhere (e.g. Portu et al., 2015). Tissue sections (~30 μm thickness) were obtained from frozen tissue (cryosectioning) with a cryostatic microtome Leica Microsystems CM 1850 and mounted on polycarbonate foils. The biological samples were processed the same as the standards.

3. Results and discussion

The obtained values of track density and average area for Exposure calculation were estimated as $\rho = 0.019 \mu\text{m}^{-2}$, A_t (4 min etching) = 2.75 μm² and A_t (5 min etching) = 3.59 μm² respectively.

In Fig. 2, the OD results obtained using NG measurements for both 4 and 5 min etching time were plotted together with curves calculated using Eq. (3), the expression corresponding to thick detectors in the model proposed by Ilic and Najzer (1990a), which is the actual case.

In the range $0,03 < E < 3$, where OD measurements were performed, experimental points have approximately the same tendency as the curves calculated with the model. Besides, when plotted as a function of Exposure, experimental points corresponding to 4 and 5 min etching time get aligned on the same curve, for both SLCs and agarose samples. On the other hand, SLCs results fit better the theoretical curve than the agarose gel ones. It was also found that agarose gels had some handling difficulties (preparation times, drying, etc) which impact on the reproducibility of the images. From the above, and due to the better repeatability and constancy of the SLCs standards, it was decided to use these ones to perform the calibration curve. Results of boron concentration as a function of OD, obtained for SLCs standards, show a linear response in the range between 0 and 200 ppm, as shown in Fig. 3. Each experimental point is calculated using the mean value of NG measured over 10 photographs and the error is computed using the standard deviation of these measurements.

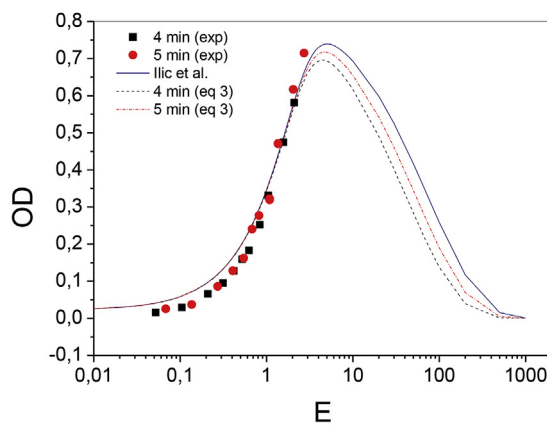
Fitting of this calibration curve leads to equation (4) by the inverse prediction procedure (Rice, 1995)

$$[^{10}\text{B}] = 329.33 \text{ OD} - 2.13 \quad R^2 = 0.9945 \quad (4)$$

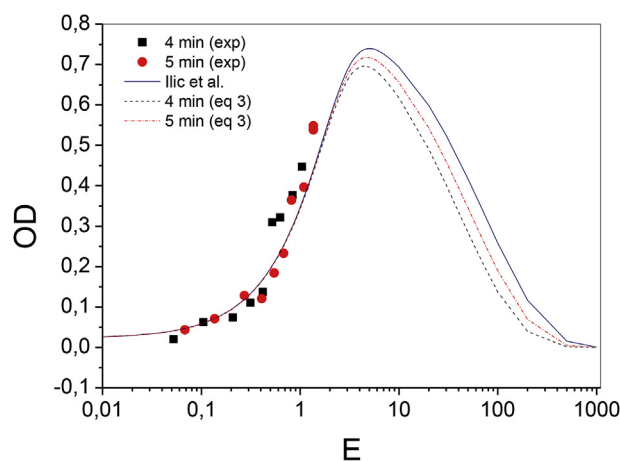
where OD is calculated as the logarithm of the grey level of a control image (an image of untreated Lexan acquired at the same conditions as that of the sample or pattern to be measured) divided the grey level of the ROI. It should be noted that linearity of OD in this boron concentration range is essential to quantify boron content in unknown samples. In fact this calibration curve allows the measurement of boron concentration in most of tissue samples coming from BNCT protocols.

An example of boron concentration determination in different regions of a tissue sample is presented in Fig. 4. The microphotograph of a premalignant tissue section of hamster cheek pouch (hamster cheek pouch model, Kreimann et al., 2001) and its corresponding autoradiographic image are shown.

Values of boron concentration in the ROIs of the figure were



a)



b)

Fig. 2. Experimental data and calculated curves of Optical Density as a function of Exposure for a) aqueous solutions of enriched boric acid (99%) in SLCs; b) Low Melting point agarose gel. The curve “Ilic et al.” corresponds to the theoretical curves calculated with values reported by Ilic et al.

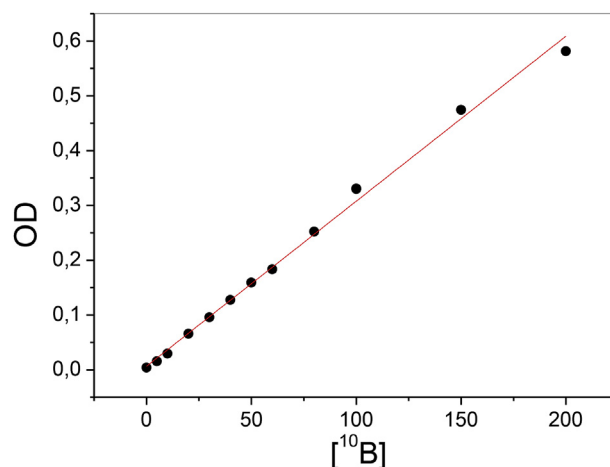


Fig. 3. Calibration curve: Aqueous solutions of enriched boric acid (99%) in Small Lexan™ Cases. Boron concentration values between 0 and 200 ppm. Error bars cannot be distinguished because of their small amplitudes.

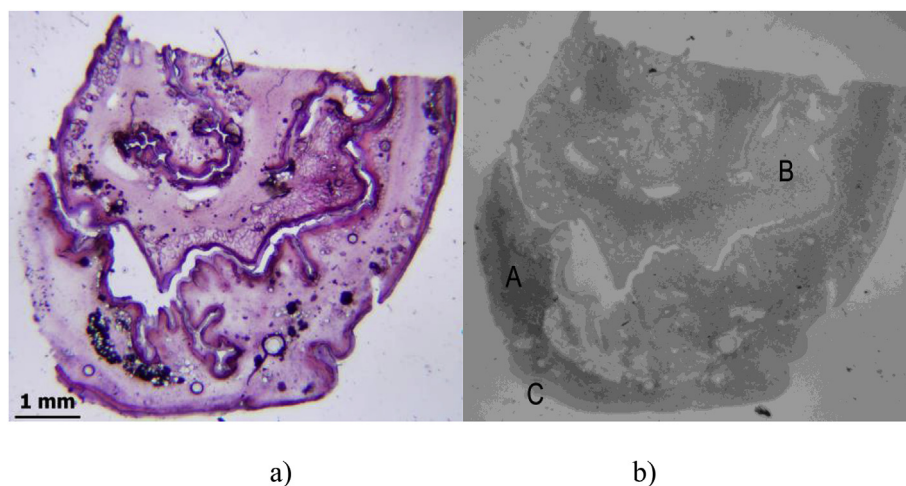


Fig. 4. a) Premalignant tissue section of hamster cheek pouch. Hamster infused with GB-10 (50 mg kg^{-1}). b) Autoradiography image. A: Connective tissue, B: muscle, C: Epithelium. Original magnification: $1.25\times$.

determined using BNCT-AR, which includes the calibration curve shown above (Equation (4)). The estimated values are: $14 \pm 1 \text{ ppm}$ in connective tissue, $6 \pm 1 \text{ ppm}$ in muscle, and $11 \pm 1 \text{ ppm}$ in epithelium. These results are in accordance with previously reported measurements obtained in QTA by track counting (Portu et al., 2015).

4. Conclusions

OD calculated from grey levels NG measured with the BNCT-AR code proved to be a suitable parameter to determine boron concentration between 0 and 200 ppm.

Optical density values measured in SLCs in a range of exposure E $0.03 < E < 3$ showed a similar behavior to curves proposed in Ilic and Najzer (1990a) model.

SLCs standards were used to perform a calibration curve, and boron concentration could be determined in regions of interest of a tissue section from an experimental model. The methodology proposed in this work using the code BNCT-AR would allow a fast preliminary analysis of histological and autoradiographic images in the different regions of interest of samples of interest for BNCT. If necessary, a QTA deeper analysis can then be performed.

Acknowledgements

The authors acknowledge Dr. Schwint and coworkers for providing biological samples. This work was partially supported by a Medical research grant for young researchers from A. J. Roemmers Foundation, Argentina.

Appendix A. Supplementary data

Supplementary data to this article can be found online at <https://doi.org/10.1016/j.radmeas.2018.10.005>.

References

Futamura, G., Kawabata, S., Siba, H., Kuroiwa, T., Suzuki, M., Kondo, N., Ono, K., Sakurai, Y., Tanaka, M., Todo, T., Miyatake, S.I., 2014. A case of radiation-induced osteosarcoma treated effectively by boron neutron capture therapy. *Radiat. Oncol.* 9, 237.

González, S.J., Bonomi, M.R., Santa Cruz, G.A., Blaumann, H.R., Calzetta Larriou, O.A., Menéndez, P., Jiménez Rebagliati, R., Longhino, J., Feld, D.B., Dagrosa, M.A., Argerich, C., Castiglia, S.G., Batistoni, D.A., Liberman, S.J., Roth, B.M., 2004. First BNCT treatment of a skin melanoma in Argentina: dosimetric analysis and clinical outcome. *Appl. Radiat. Isot.* 61 (5), 1101–1105.

Ilic, R., Najzer, M., 1990a. Image formation in track-etch detectors I - the large area signal transfer function. *Nucl. Tracks Radiat. Meas.* 17 (4), 453–460.

Ilic, R., Najzer, M., 1990b. Image formation in track-etch detectors II - the space-dependent transfer function in thin detectors. *Nucl. Tracks Radiat. Meas.* 17 (4), 461–468.

Kankaanranta, L., Seppälä, T., Koivunoro, H., Saarihahti, K., Atula, T., Collan, J., Salli, E., Kortensniemi, M., Uusi-Simola, J., Välimäki, P., Mäkitie, A., Seppänen, M., Minn, H., Revitzer, H., Kouri, M., Kotiluoto, P., Seren, T., Auterinen, I., Savolainen, S., Joensuu, H., 2012. Boron neutron capture therapy in the treatment of locally recurrent head-and-neck cancer: final analysis of a phase I/II trial. *Int. J. Radiat. Oncol. Biol. Phys.* 82 (1), e67–75.

Kato, I., Ono, K., Sakurai, Y., Ohmae, M., Maruhashi, A., Imahori, Y., Kirihata, M., Nakazawa, M., Yura, Y., 2004. Effectiveness of BNCT for recurrent head and neck malignancies. *Appl. Radiat. Isot.* 61 (5), 1069–1073.

Kreimann, E.L., Itoiz, M.E., Dagrosa, A., Garavaglia, R., Farias, S., Batistoni, D., Schwint, A.E., 2001. The hamster cheek pouch as a model of oral cancer for boron neutron capture therapy studies: selective delivery of boron by boronophenylalanine. *Cancer Res.* 61, 8775–8781.

Moss, R.L., 2014. Critical review, with an optimistic outlook, on boron neutron capture therapy (BNCT). *Appl. Radiat. Isot.* 88, 2–11.

Portu, A., Bernalda, O.A., Nievas, S., Liberman, S., Saint Martin, G., 2011a. Measurement of ^{10}B concentration through autoradiography images in polycarbonate nuclear track detectors. *Radiat. Meas.* 46, 1154–1159.

Portu, A., Saint Martin, G., Brandizzi, D., Bernalda, O.A., Cabrini, R.L., 2011b. ^{10}B concentration evaluation in autoradiography images by optical density measurements. *Appl. Radiat. Isot.* 69, 1710–1712.

Portu, A., Carpano, M., Dagrosa, A., Cabrini, R.L., Saint Martin, G., 2013. Qualitative autoradiography with polycarbonate foils enables histological and track analyses on the same section. *Biotech. Histochem.* 88 (5), 217–221. <https://doi.org/10.3109/10520295.2012.759624>.

Portu, A., Molinari, A.J., Thorp, S.I., Pozzi, E.C.C., Curotto, P., Schwint, A.E., Saint Martin, G., 2015. Neutron autoradiography to study boron compound micro-distribution in an oral cancer model. *Int. J. Radiat. Biol.* 91 (4), 329–335.

Rice, J., 1995. *Mathematical Statistics and Data Analysis*, second ed. Duxbury Press.

Skvarc, J., Ilic, R., Yanagie, H., Rant, J., Ogura, K., Kobayashi, H., 1999. Selective radiography with etched track detectors. *Nucl. Instrum. Methods Phys. Res. B* 152, 115–121.

Suzuki, M., Sakurai, Y., Masunaga, S., Kinashi, Y., Nagata, K., Maruhashi, A., et al., 2006. Feasibility of boron neutron capture therapy (BNCT) for malignant pleural mesothelioma from a viewpoint of dose distribution analysis. *Int. J. Radiat. Oncol. Biol. Phys.* 66, 1584–1589.

Swinehart, D.F., 1962. The Beer-Lambert law. *J. Chem. Edu.* 39 7, 333–335.

Vidal, C., Portu, A., Saint Martin, G., 2015. Desarrollo de un sistema informático integral para el análisis de muestras histológicas – autorradiográficas en el marco de la terapia por captura neutrónica en boro. XLII Reunión Anual de la AATN (Asociación Argentina de Tecnología Nuclear) Dec. 2015.

Wang, L.W., Wang, S.J., Chu, P.Y., Ho, C.Y., Jiang, S.H., Liu, Y.W.H., Liu, Y.H., Liu, H.M., et al., 2011. BNCT for locally recurrent head and neck cancer: preliminary clinical experience from a phase I/II trial at TsingHua Open-Pool Reactor. *Appl. Radiat. Isot.* 69 (12), 1803–1806.

Yanagie, H., Higashi, S., Seguchi, K., Ikushima, I., Fujihara, M., Nonaka, Y., Oyama, K., Maruyama, S., Hatae, R., Suzuki, M., Masunaga, S., Kinashi, T., Sakurai, Y., Tanaka, H., Kondo, N., Narabayashi, M., Kajiyama, T., Maruhashi, A., Ono, K., Nakajima, J., Ono, M., Takahashi, H., Eriguchi, M., 2014. Pilot clinical study of boron neutron capture therapy for recurrent hepatic cancer involving the intra-arterial injection of a (^{10}B) -containing WOW emulsion. *Appl. Radiat. Isot.* 88, 32–37.

Zonta, A., Prati, U., Roveda, L., Ferrari, C., Zonta, S., Clerici, A.M., Zonta, C., Pinelli, T., Fossati, F., Altieri, S., Bortolussi, S., Bruschi, P., Nano, R., Barni, S., Chiari, P., Mazzini, G., 2006. Clinical lessons from the first applications of BNCT on unresectable liver metastases. *JPCS* 41, 484–495.